

1 **Is Annual Recharge Coefficient a Valid Concept in Arid and Semi-Arid Region?**

2
3 A manuscript submitted to *Hydrology and Earth System Sciences*

4 By

5 Yiben Cheng^{ab*}, Hongbin Zhan^{b*}, Wenbin Yang^{a*}, Hongzhong Dang^a, Wei Li^a

6
7 ^a Institute of Desertification Studies,

8 Chinese Academy of Forestry,

9 Haidian District, Beijing 100093, P. R. China (chengyiben07@gmail.com)

10
11 ^bDepartment of Geology & Geophysics,

12 Texas A&M University,

13 College Station, TX 77843-3115, USA. (zhan@geos.tamu.edu)

14
15 *Co-corresponding authors

16
17
18
19 March, 2017

21 **Abstract.** Deep soil recharge (DSR) (at depth more than 200 cm) is an important part of water
22 circulation in arid and semi-arid regions. Quantitative monitoring of DSR is of great importance
23 to assess water resources and to study water balance in arid and semi-arid regions. This study
24 used a typical bare land on the Eastern margin of Mu Us Sandy Land in the Ordos basin of China
25 as an example to illustrate a new lysimeter method of measuring DSR to examine if the annual
26 recharge coefficient is valid or not in the study site, where the annual recharge efficient is the
27 ratio of annual DSR over annual total precipitation. Positioning monitoring was done on
28 precipitation and DSR measurements underneath mobile sand dunes from 2013 to 2015 in the
29 study area. Results showed that use of an annual recharge coefficient for estimating DSR in bare
30 sand land in arid and semi-arid regions is questionable and could lead to considerable errors. It
31 appeared that DSR in those regions was influenced by precipitation pattern, and was closely
32 correlated with spontaneous strong precipitation events (with precipitation greater than 10 mm)
33 other than the total precipitation. This study showed that as much as 42% of precipitation in a
34 single strong precipitation event can be transformed into DSR. During the observation period,
35 the maximum annual DSR could make up 24.33% of the annual precipitation. This study
36 provided a reliable method of estimating DSR in sandy area of arid and semi-arid regions, which
37 is valuable for managing groundwater resources and ecological restoration in those regions. It
38 also provided strong evidence that the annual recharge coefficient was invalid for calculating
39 DSR in arid and semi-arid regions. This study shows that DSR is closely related to the strong
40 precipitation events, rather than to the average annual precipitation, as well as the precipitation
41 patterns.

42 **Key words:** Deep soil recharge, deep soil infiltrometer, sandy land, new apparatus, rainfall,
43 lysimeter

45 **Introduction**

46 Recharge is an important source of groundwater budget and it is also a fundamental process
47 that links the surface hydrological processes (e.g. precipitation), vadose zone process (e.g.
48 infiltration and soil moisture dynamics), and the saturated zone process (e.g. groundwater flow)
49 (Sanford, 2002;McWhorter and Sunada, 1977). How to accurately estimate recharge remains a
50 persistent challenge and an active research topic in the hydrological science community over
51 many decades (Gee and Hillel, 1988;Scanlon, 2013;Sanford, 2002). It is generally accepted that
52 recharge is correlated to the precipitation in some fashions, and many studies adopt the concept
53 of a recharge coefficient (Turkeltaub et al., 2015;Kalbus et al., 2006;Allocca et al., 2014), which
54 is the ratio of the actual recharge to the precipitation, to estimate the recharge (Fiorillo et al.,
55 2015;Allocca et al., 2014). The magnitude of such a recharge coefficient is controlled by a
56 complex interplay of multiple factors such as moisture dynamics in the vadose zone
57 (Schymanski et al., 2008), depth to water table, vegetation, etc., and the recharge coefficient is
58 often regarded as a temporally invariant value at a given location (Fiorillo et al., 2015;Min et al.,
59 2017;Vauclin et al., 1979). Specifically, it is assumed to be primarily controlled by the total
60 precipitation, not too much by the temporal fluctuation of precipitation events (Hickel and Zhang,
61 2006;Acworth et al., 2016). In this study, we will challenge the concept of using a constant
62 recharge coefficient to estimate the recharge in arid and semi-arid regions based on a multi-year
63 field investigation.

64 As water tables in many arid and semi-arid regions are relatively deep (greater than 2
65 meters below ground surface) (Williams, 1999;Soylu et al., 2011), recharge in those regions is
66 named Deep Soil Recharge (DSR), which will be the concern of this study. DSR could ease the
67 demand of sand-fixing vegetation on moisture during extremely dry seasons (Zhang et al.,

68 2001;Shou et al., 2016) , and it reduces water deficit, sustains life activities, and helps the
69 vegetation live through extreme droughts (Zhang et al., 2004). In this sense, DSR is an important
70 factor of water cycle in arid and semi-arid regions (Adolph, 1947), and it could also provide
71 much needed references for the stability analysis of sand-fixing vegetation (Li et al., 2004;Li et
72 al., 2014). In the following, we will briefly review the existing methods of estimating DSR.

73 In general, there are three methods of measuring DSR in arid and semi-arid regions. The
74 first is an empirical approach which assigns a constant recharge coefficient associated with a
75 certain precipitation event (Allison et al., 1994;Jiménez-Martínez et al., 2010). The empirical
76 approach is simple to use but it lacks a rigorous theoretical base, and the recharge coefficient has
77 to be calibrated through a groundwater flow model in the region, which is often not available.

78 The second is a modeling approach involving numerical models such as HYDRUS
79 (Šimůnek et al., 2012), SWAT (Arnold et al., 2012), UNSATH (Fayer, 2000), SWIM
80 (Krysanova et al., 2005), SWAP (van Dam, 2000) to calculate DSR. Modeling is an efficient
81 way to test different hypothetical scenarios and it may be used to predict DSR in the future if the
82 model is calibrated carefully. Detailed water balance models can be used for irrigated
83 agriculture, but they usually cannot predict evapotranspiration accurately, especially when plants
84 suffer seasonal water stress and plants cover is sparse (Gee and Hillel, 1988). When recharge is
85 estimated as residual in water balance models, it can cause miscalculation as much as an order of
86 magnitude (Scanlon, 2013;Voeckler et al., 2014). When using soil water flow models with
87 measured or estimated soil hydraulic conductivities and tension gradients, similar miscalculation
88 can also occur (Nyman et al., 2014;Gee and Hillel, 1988). In addition, the modeling usually
89 involves upscaling of parameter values over a spatially and temporally discretized mesh from
90 measurements which are made on specific moments and locations. Such an upscaling process is

91 not always easy to execute and it could sometimes lead to serious errors. This is particularly true
92 for arid and semi-arid regions where most precipitation may be episodic (occurring in short and
93 unpredictable events) (Modarres and da Silva, 2007;Zhou et al., 2016), and may be confined to
94 restricted portions of the area (Gee and Hillel, 1988).

95 The third includes a cluster of experimental techniques such as isotopic tracer (Klaus and
96 McDonnell, 2013), water flux (Katz et al., 2016), and lysimeter (Scanlon, 2013). Among them,
97 lysimeters are instruments that directly measure the hydrological cycle in infiltration, runoff and
98 evaporation. Generally, this instrument is located in an open observation field or as a controlled
99 device, working either solely or in groups (Good et al., 2015). In a typical lysimeter, soil are
100 filled into a column surrounded by impermeable lateral boundaries thus water can only enter or
101 leave the column from upper or lower boundaries (Duncan et al., 2016;Fritzsche et al., 2016). A
102 drainage system is usually placed at the bottom (Glenn et al., 2013). The depth of soil in the
103 column depends on the experimental purpose. Experiments can be done with the same type of
104 soil at different depths in a single column, or in different columns but at the same depth. The soil
105 surface can be cultivated with different crops or left as bare land. Observation can be recorded
106 with weight or volume of water.

107 Application of above-mentioned methods for assessing DSR in arid and semi-arid regions
108 has met a variety of challenges, primarily due to the fact that precipitation events often happen in
109 the form of short pulses with highly variable intensity (Collins et al., 2014). The intermittent and
110 unpredictable characteristics of precipitation events lead to highly variable moisture and nutrient
111 levels in the soils (Beatley, 1974;Huxman et al., 2004). It is unclear how the precipitation
112 amount, time, and interval will affect the water moisture of arid and semi-arid regions, especially
113 the change of deep soil water storage.

114 In this study, a new type of lysimeter is designed to accurately measure the amount of DSR
115 in arid and semi-arid regions. With the help of a three-year (2013-2015) field investigation with
116 this new lysimeter, one can answer the following question: Is the concept of an annual recharge
117 coefficient valid or not for estimating DSR at a given location in an arid and semi-arid region?
118 Before the introduction of this new type of lysimeter, it is necessary to briefly explain the
119 challenges faced by the conventional lysimeter for studying DSR in arid and semi-arid regions.

120 **2. Design of the new lysimeter for DSR measurement**

121 **2.1. Problems with the conventional lysimeter methods in arid and semi-arid regions**

122 Lysimeters have been used to access the amount of water consumed by vegetation for more
123 than three hundred years (Howell et al., 1991). The type of lysimeter that is specifically designed
124 to measure evapotranspiration (ET), called precision weighing lysimeter, has been developed
125 within the past six decades. In order to satisfy different requirements and needs, there are various
126 designs of weighing lysimeters, with surface areas ranging from 1.0 m² to over 29 m² (Howell et
127 al., 1991). The stored media mass and the type of scale such as diameter and height are factors
128 on which the accuracy of ET measurement depends, and many lysimeters have accuracy better
129 than 0.05 mm (Howell et al., 1991). Figure 1A shows the schematic diagram of a conventional
130 lysimeter installation in the field. It is basically a weight meter of soil with an open upper
131 boundary at ground surface and a perforated bottom boundary and impermeable vertical side
132 walls. The typical depth of lysimeters varies from 0.2 m to 2 m, but is rarely greater than 2.5 m
133 (Howell et al., 1991). The horizontal cross-section area is usually in the range of 1 m² to 29 m².
134 Precipitated water can freely infiltrate into the soil from the top and downward flow of water at
135 the bottom of the lysimeter is collected (through the perforation) as a function of time to
136 calculate the recharge. Alternatively, the weight of combined water and soil inside the lysimeter

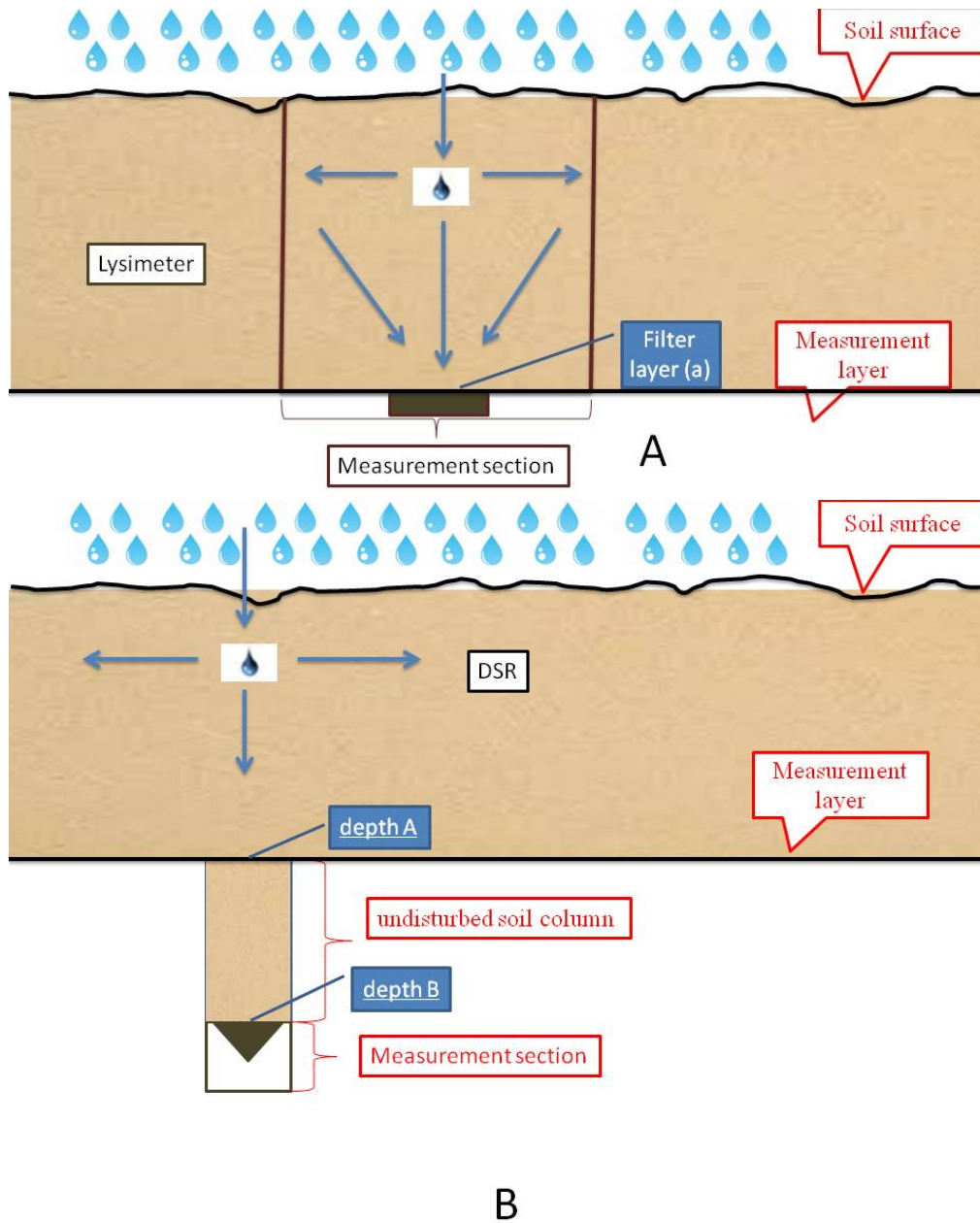
137 can be accurately measured using a weight gauge to reflect any soil moisture change. Such
138 information, combined with infiltration or evaporation at the surface, can yield the information
139 of downward water flux at the depth of lysimeter.

140 The following issues deserve special attention when applying the conventional lysimeter for
141 measuring recharge. Firstly, soil layers are inevitably disturbed when installing the instrument,
142 so the result may not reflect the actual recharge in native (undisturbed) soils (Weihermüller et al.,
143 2007) . Secondly, the cost is too high to use multiple lysimeters to observe large-scale infiltration
144 (Stessel and Murphy, 1992). Thirdly, when precipitation strength is relatively light and
145 concentrated, a large lysimeter cannot sensitively and rapidly measure DSR (Goldhamer et al.,
146 1999;Farahani et al., 2007). The conventional lysimeter often cannot answer the following
147 questions: To what soil layer can different levels of precipitations infiltrate? How much is the
148 infiltration amount under different levels of precipitation? (Gee and Hillel, 1988;Ogle and
149 Reynolds, 2004).

150 The conventional lysimeter as shown in Figure 1A may meet additional challenges when
151 applied to arid and semi-arid regions. Firstly, the water table depths in arid and semi-arid regions
152 may be much greater than the maximal depth of a conventional lysimeter (2.5 m). For instance,
153 in Chagan Nur, southeast of Mu Us sandy land in the Ordos basin of China, the water table depth
154 was found to be greater than 4 m. In the Gobi desert, the water table was reported to be at least
155 2.8 m deep (Ma et al., 2009). Therefore, the infiltration measured at the base of a conventional
156 lysimeter may not represent the actual recharge that eventually enters the groundwater system.
157 Secondly, the measurement accuracy of lysimeter often declines for soils with deep plant roots
158 because the depth of lysimeter installation is limited and it may be less than the depth of those
159 roots at site, which by itself can be important pathways for water migration. Consequently, the

160 measured recharge of such disturbed soil by lysimeter may not represent the in-situ recharge of
161 the native (undisturbed) soil.

162 To resolve the above-mentioned issues faced by the conventional lysimeter, a new type of
163 lysimeter is designed with specific considerations of the unique precipitation patterns and soil
164 characteristics in arid and semi-arid regions. This new lysimeter is illustrated schematically in
165 Figure 1(B).



166

167

168 Figure 1. Schematic diagram of conventional lysimeter (A) and the new lysimeter (B).

169 **2.2 Design of a new lysimeter for measuring DSR in arid and semi-arid regions**

170 This new lysimeter has a few innovations (see Figure 1B) that can be outlined as follows.

171 Instead of setting the upper boundary of the lysimeter at ground surface, the new design has its

172 upper boundary at a designed depth (denoted as depth-A in Figure 1B) where infiltration will be

173 measured. A cylindrical container with a diameter of 20 cm to 40 cm with impermeable walls is
174 installed from depth-A downward to a deeper depth-B. The length of AB is determined
175 according to the capillary rise of the in-situ soil, which can be calculated using the average grain
176 size of soils within AB. More specifically, the length of AB is greater than the capillary rise of
177 soils within AB and it is usually great than 0.6 m (Liu et al., 2014). At the soil surface there is a
178 device to measure the amount of the precipitation and at the base of the instrument (depth B), a
179 water collection device is used to measure the amount of water exit the base.

180 Before the measurement, one necessary preparation is to inject water from the top of the
181 instrument at depth-A using water pumps, the injection will stop until water starts to drip out
182 from the base at depth-B. One usually has to wait 10 days to allow the water profile in column
183 AB to become equilibrium. When water stops flowing out from depth-B, the soil water in the
184 column is regarded as reaching its equilibrium state, in which the soil moisture at depth-B
185 reaches the maximum field capacity. Under such an equilibrium status, the amount of infiltration
186 entering the upper surface of the lysimeter will be discharged (with the same amount) from the
187 base of the lysimeter after a certain delay time.

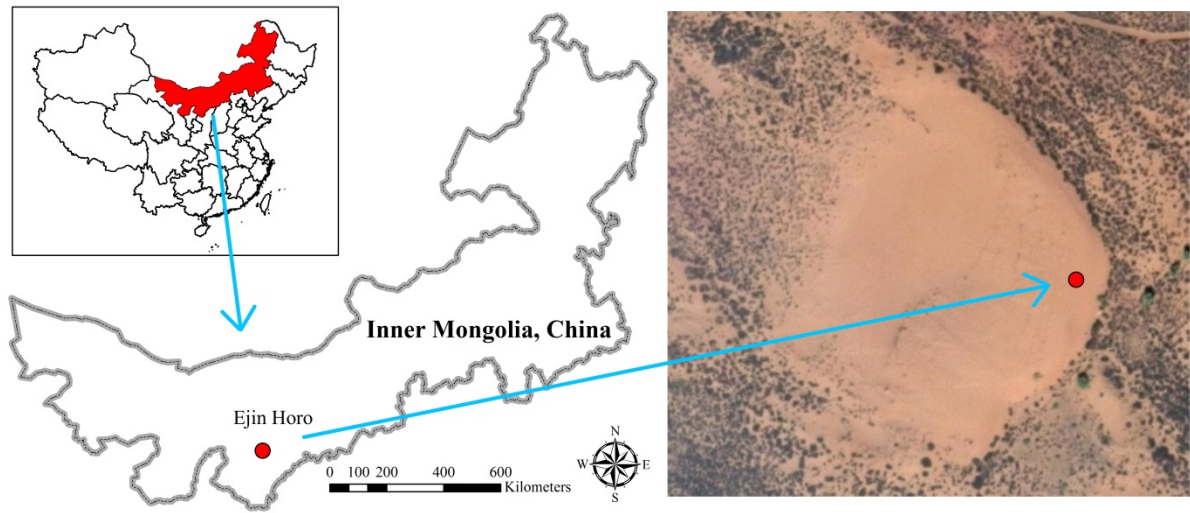
188 The proposed new method has a few innovative features that have not been considered in
189 previous studies. Firstly, it can measure DSR at any given layer of a multi-layer soil system
190 using a single apparatus installed in the field. Secondly, continuous real-time measurements can
191 be recorded over any given time period, thus a time-series of DSR can be obtained, which will be
192 very useful to understand the soil water dynamics at sandy area of arid and semi-arid regions.
193 Thirdly, the apparatus is portable and easy to install, thus a large amount of data can be collected
194 in various locations of a study area using multiple lysimeters, and spatial recharge distribution
195 can also be obtained straightforwardly. This method is field tested in arid and semi-arid sandy

196 regions of western China. It provides key references for the evaluation of water resources, water
197 balance, and the stability assessment of sand-fixing vegetation in arid and semi-arid areas. It also
198 provides data that are much needed for evaluating soil water contents and groundwater resources
199 of those areas. An important feature of this new lysimeter is that it can provide reliable DSR data
200 to examine the concept of annual recharge coefficient when comparing with the precipitation
201 data.

202 **3. Field testing of the new apparatus**

203 **3.1 Description of the study area**

204 Figure 2 shows the location of the study which is located in Ejin Horo Banner, on the
205 Eastern margin of Mu Us Sandy Land in the Ordos basin of China (geographic location: 39°05'
206 N, 109°36' E; altitude: 1070-1556 m above mean sea level). The groundwater table between
207 dunes are 5.3-6.8 m below ground surface. The climate is semi-arid continental monsoon climate
208 zone. Precipitation concentrates from July to September, with relatively concentrated rainstorm.
209 The average annual precipitation from 1960 to 2010 is 296.01 mm. The average annual
210 temperature of this area is 6.5°C, with about 151 days of frost-free season, 1809 mm total
211 evaporation, an average of 2900 hours of sunshine, and an average wind speed of 3.24 m/s (Wu
212 and Ci, 2002; Karnieli et al., 2014). The study area is located in relatively gentle mobile dunes,
213 and the soil type is Aeolian sandy soil.



214



215

216

Figure 2. Geographic location of the experimental area.

217

In term of geological structure, Mu Us Sandy Land is in the Ordos basin, a large-scale

218

syncline sedimentary basin with nearly north-south striking axis, and is of Mesozoic and

219

Paleozoic ages. The basin covers an area of 640 km from north to south, and 400 km from east to

220

west. The axis of syncline is off west, and the east and west wings are asymmetric. The east wing

221

is Monoclinic of westward tilt with a width of more than 300 km. The west wing is made of

222 many fault-fold belts striking along the north-south direction and thrusting eastward with a width
223 of less than 100 km. The southern boundary of the basin is Weibei plateau uplift. The southern
224 part of this plateau uplift is descending in ladder-shape with blocks to Fenwei rift-subsidence
225 basin. The northern boundary of this basin is Yimeng plateau uplift, with a lack of Lower
226 Paleozoic, and its edge-fault is connected to Hetao fault basin. The basement of Ordos basin is of
227 Precambrian crystalline metamorphic rocks.

228 Deposited in the basin are, in turn, Lower Paleozoic carbonate rocks, Upper Paleozoic-
229 Mesozoic clastic rocks, and Cenozoic sedimentary rocks with a total depth of more than 6000 m.
230 The discontinuous Cenozoic sediment is on top of the Mesozoic and Paleozoic layers, mainly of
231 the Quaternary and partially of the Tertiary sediments. The Quaternary layer is mainly made of
232 Aeolian sand and loess. Generally divided by a line along the Great Wall, the northwest land
233 surface is mainly covered by wind-blown sand layers of varying thickness and a 40-120 m thick
234 layer of alluvial-lacustrine; the southeast land surface is mainly covered by loess with various
235 thickness from tens of meters to more than 200 m. Below the loess layers, there is Tertiary
236 Pliocene mud rock with thickness of a few meters to tens of meters.

237 The hydro-stratigraphic units of the Ordos basin is quite complex, consisting of multiple
238 connected aquifers. Following the order from bottom to top, the multiple aquifers are primarily
239 made from various rock types of a karst aquifer consisting of Precambrian and Ordovician
240 limestone, a fractured aquifer consisting of Carboniferous and Jurassic clastic rocks, a porous-
241 fractured aquifer of Cretaceous clastic rocks, and a porous aquifer consisting of unconsolidated
242 Cenozoic and Quaternary sediments. Generally speaking, Mu Us Sandy Land has relatively rich
243 groundwater resources. The shallow groundwater reservoir is estimated to hold about 120.3
244 billion metric tons of freshwater. Groundwater is mainly recharged by precipitation with an

245 annual average recharge amount of 1.4 billion metric tons. Fine sands are the dominating
246 sediments observed in the experimental site. In the upper 200 cm soil layer in the experiment
247 area, the percentage of fine sand (0.5-0.1 mm) are 88.56%, 77.88%, 88.23%, 88.89%, 90.28%,
248 83.90%, and 84.21% at depths of 0 cm, 10 cm, 30 cm, 60 cm, 90 cm, 150 cm, and 200 cm,
249 respectively. The rest parts of the soil are primarily coarse sands. It is evident that the soil at the
250 upper 200 cm is relatively homogeneous.

251 **3.2 Statistical analysis of data**

252 Research on the relationship between precipitation and DSR of bare sand land in arid and
253 semi-arid regions is beneficial to understand the soil-water dynamics of those regions. Because
254 vegetation is absent, complexity related to transpiration process by plants is not a concern.
255 Based on two time series of real-time data of precipitation and DSR, one can examine the
256 relationship between DSR and precipitation. This study can serve as a basis for further study of
257 DSR in semi-fixed and fixed sand lands with different fractional vegetation covers.

258 In September 1, 2012, a mobile sand dune within the study site was set as the monitoring
259 plot (geographic location: 39°05' N, 109°36' E; altitude: 1310 m) with the upper 300 cm soil
260 profile excavated. The lysimeter as shown in Figure 1B was installed following the procedure
261 described in section 2.2 and then backfilled using the excavated soil. Infiltration passing through
262 the upper 200 cm depth is generally regarded as DSR in this study. It is worthwhile to point out
263 that some other investigators may use a more or less different depth threshold for defining DSR.
264 For instance, (Zhang et al., 2008) used 140 cm instead of 200 cm depth as the threshold to define
265 DSR. It was found that the water table depth was greater than 5 m in 2012-2015 at the study site,
266 so its influence to DSR was negligible. A precipitation sensor (AV-3665R, AVALON, United
267 States; precision: 0.2 mm) was placed above ground at the site. Data acquirer (CR200X,

268 Campbell, USA) was used to record DSR, of which DSR data were recorded every one hour, and
 269 the precipitation data were recorded every half hour. In order to avoid the effect of freeze-and-
 270 thaw action, the experiment was conducted between April 1, 2013 and November 30, 2015.
 271 During such a three-year period, no runoff occurs at the studied area.

272 The statistics of precipitation and DSR are shown in Table 1, which reveals that there is an
 273 obvious difference of precipitation at the experimental plot from 2013 to 2015. The annual
 274 precipitation is 83 mm in 2013, 205.6 mm in 2014, and 186.4 mm in 2015. This is to say, the
 275 annual precipitations in 2014 and 2015 are 2.48 and 2.25 times of that in 2013, respectively.
 276 Such a dramatic fluctuation and uneven distribution of annual precipitation is typical of arid and
 277 semi-arid regions. The corresponding annual DSR is 20.2 mm in 2013, 20.6 mm in 2014, and 9.2
 278 mm in 2015. This is to say that the annual DSR values in 2014 and 2015 are 1.02 and 0.46 of that
 279 in 2013. The annual DSR/precipitation ratios (or the so-called annual recharge coefficient) for
 280 2013, 2014, and 2015 are 24.33%, 10%, and 4.94%, respectively.

281 It appears that there is no clear correlation between the annual DSR and the annual
 282 precipitation according to the data of 2013-2015. In another words, use of the annual recharge
 283 coefficient for the study site becomes questionable as such a coefficient implies that there is a
 284 close correlation between the annual DSR and the annual precipitation, which is not supported
 285 by the data of 2013-2015 here. Therefore, we will scrutinize the precipitation pattern and
 286 intensity more closely to decipher the connection of precipitation and DSR in the following.

287 Table 1: The annual precipitation-DSR relationship from 2013-2015.

Year	Precipitation (mm)	DSR (mm)	DSR/precipitation*100%
------	-----------------------	-------------	------------------------

2013	83	20.2	24.33%
2014	205.6	20.6	10%
2015	186.4	9.2	4.94%

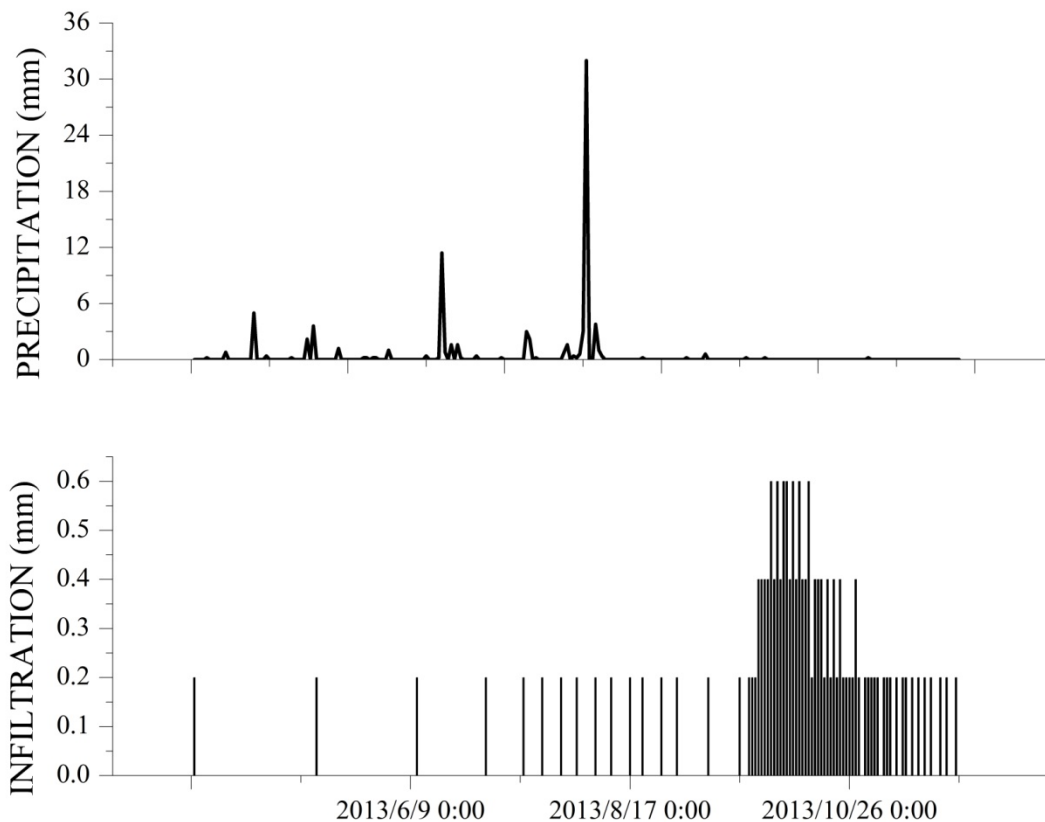
288

289 **3.2.1 The relationship between precipitation pattern and DSR**

290 Research on bare sandy soil water dynamic process usually focuses on temporal and vertical
 291 differences (Ritsema and Dekker, 1994; Postma et al., 1991). In terms of temporal soil moisture
 292 variation over an annual cycle, the process could be divided as soil moisture replenishment,
 293 depletion, and relatively stable periods. In term of vertical soil moisture variation, soil water
 294 content usually first increases with depth and then decreases based on an interplay of mutual
 295 infiltration and evaporation processes. In general, soil could be divided as a surface dry sand
 296 layer, a layer with drastic moisture change, and a layer with relatively stable moisture content.
 297 Specifically, the soil deeper than 160 cm in arid and semi-arid regions would have a relatively
 298 stable moisture content. This is because of two reasons. Firstly, soil water will not be up-taken to
 299 the surface by capillary force at such depths; secondly, ground water table in arid and semi-arid
 300 regions is usually much lower than 160 cm.

301 In our study site, 2013 is an especially dry year with only 83 mm precipitation compared to
 302 296.01 mm of average annual rainfall calculated over a period from 1960 to 2010. The
 303 precipitation and DSR patterns of 2013 are shown in Figure 3. The measurement accuracy of the
 304 lysimeter is 0.2 mm. During the observation period from April 1 to November 30, there are
 305 totally 25 recorded precipitation events, mostly concentrated in the period from May to August.

306 There is a one-time strongest precipitation event with a 24-hour precipitation amount reaching 32
307 mm in August 3. The DSR correlated to this event can be identified from September 21 to
308 November 30 and reaches 17.2 mm. The delay time from precipitation event to the start of DSR
309 is approximately 48 days. The DSR/precipitation ratio for this particular event is as high as
310 53.75%. Such a DSR/precipitation ratio appears to be the highest in 2013. It is notable that
311 although the strongest precipitation event at August 3 contributes the greatest to DSR observed
312 from September 21 to November 30, a few precipitation events with amount of 6.6 mm prior to
313 this strongest precipitation event also contribute a minor part for DSR from July 27 to August 1.
314 It is also notable that the DSR/precipitation ratio for the strongest precipitation event is
315 substantially higher than the average annual recharge coefficient of 24.33% in 2013. This leads
316 to the conclusion that DSR is closely related to the strong precipitation events, rather than to the
317 average annual precipitation.



318

319

Figure 3: Precipitation and DSR patterns in 2013.

320

In 2014, the annual precipitation is 205.6 mm, and DSR is 20.6 mm, leading to a 10%

321

annual average recharge coefficient, which is less than half of that in 2013. As shown in Figure 4,

322

the frequency of precipitation events in 2014 is obviously higher than that of 2013. From April 1

323

to November 30, there are total 68 times of precipitation events, compared to 41 times in 2013.

324

Furthermore, the precipitation distribution in 2014 is more uniform than that in 2013.

325

Specifically, precipitation events are concentrated in the period from June to August, with the

326

highest 24-hour accumulative precipitation of 15 mm on July 30. As shown in Figure 4, recorded

327

DSR data cover a period from April 1 to November 30, and the maximum DSR occurs in

328

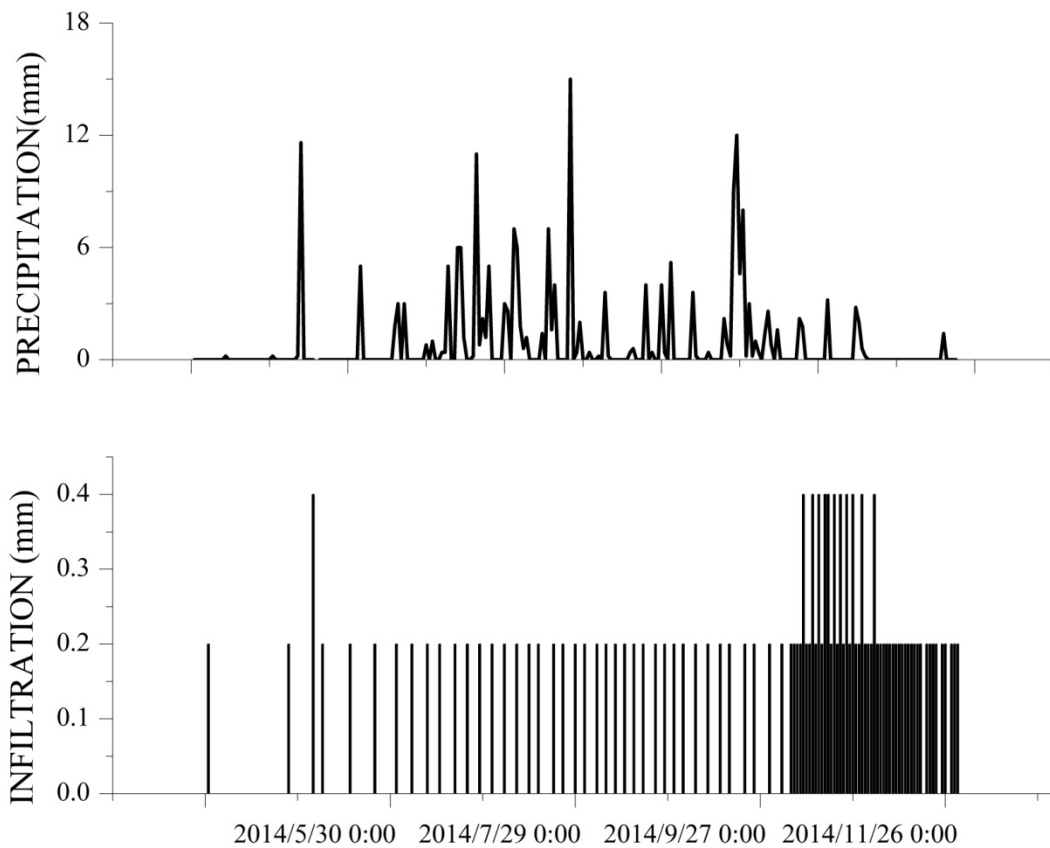
October 1. Because the experimental plot is located in a transition zone between arid and semi-

329

arid regions, summer evaporation is strong, leading to relatively less DSR during the summer

330 season. While during the period from September 1 to November 30, atmospheric temperature
331 drops and sunshine duration becomes shorter, which results in less surface evaporation and
332 greater DSR during this period. Comparing with 2013, there are more summer precipitation
333 events in 2014. That is one reason why precipitation in 2014 (205.6 mm) is greater than 2013 (83
334 mm) but the overall DSR in 2014 is less than that in 2013.

335 The strongest single-day precipitation in 2014 is 15 mm (occurred in July 30), which is less
336 than half of the strongest single-day precipitation event of 32 mm occurred in 2013 (August 3),
337 annual DSR/precipitation ratio is 24.33% in 2013 but drops to 10% in 2014. This once again
338 supports the conclusion that the strong precipitation events rather than the average annual
339 precipitation are mostly responsible for the average annual DSR. This is the other reason why
340 precipitation in 2014 (205.6 mm) is greater than 2013 (83 mm) but the overall DSR in 2014 is
341 less than that in 2013.



342

343

Figure 4: Precipitation and DSR patterns in 2014.

344

345

346

347

348

349

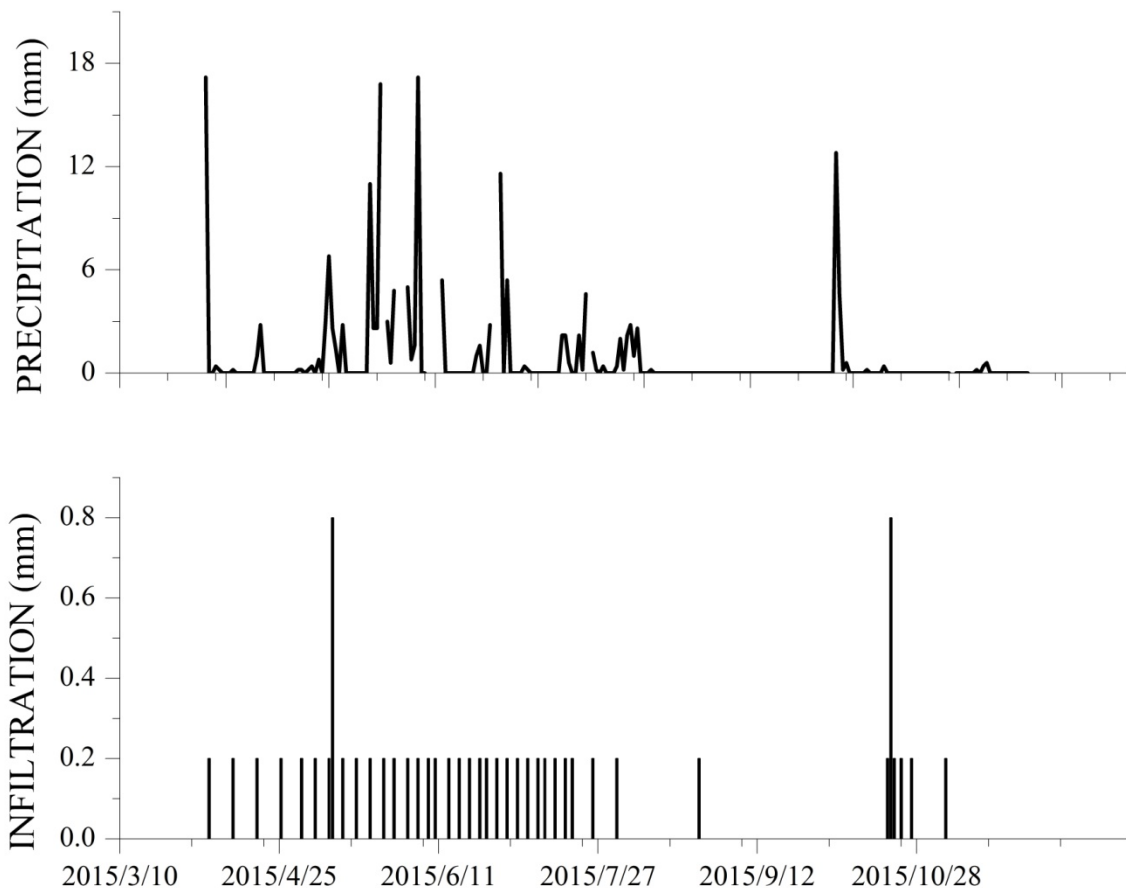
350

351

352

As shown in Figure 5, the total annual precipitation of 2015 is 186.4 mm, and DSR is 9.2 mm, leading to a 4.94% annual average recharge coefficient, which is significantly smaller than of 2013 (24.33%) and 2014 (10%). There are total 66 observable precipitation events in 2015. Such precipitation events are mostly concentrated from April 4 to July 6, with a total precipitation of 155 mm during this period, which represents 83.15% of the total precipitation in 2015. The measured DSR from April 4 to July 6 is only 7 mm, representing 77.78% of the total DSR in 2015. Throughout 2015, two strongest precipitation events happens on April 4 and June 5, both 24-hour precipitation events reach 17.2 mm. We observe a single-day DSR peak of 0.8 mm, 36 days after April 4, one of the two greatest single-day DSR values observed in 2015, but

353 no peak value of DSR response to the strong precipitation on June 5. As explained before,
 354 summer stronger evaporation leads to relatively less DSR during the summer season compared
 355 with other seasons. The third greatest precipitation is 16.8 mm on October 5, which leads to a
 356 peak value of 0.8 mm of DSR on October 21, with a 16-day delay time. If comparing the
 357 precipitation events occurred on April 4 (17.2 mm) and October 5 (16.8 mm), one can see that
 358 these two precipitation events are similar in strength (17.2 mm for April 4 and 16.8 mm for
 359 October 5) but different in the DSR delay time (36 days for April 4 and 16 days for October 5).
 360 Comparing two precipitation events which are similar in strength but different in the DSR delay
 361 time, temperature is the most likely factor responsible for such delay, so this leads to a
 362 conclusion that temperature influences the DSR rate. To investigate how the soil temperature
 363 affects the DSR rate, further field experiments are needed in the future study.



364

Figure 5: Precipitation and DSR patterns in 2015.

365
366
367
368
369
370
371
372
373
374
375
376
377
378
379
380
381
382
383
384
385
386
387

3.2.2 Relationship between precipitation intensity and DSR

Based on observational data and analysis in 3.2.1, one can see that precipitation intensity, to some extent, influences DSR. For the sake of illustration, the precipitation intensity for bare sand land is roughly classified into light, moderate, and strong events with precipitation amount less than 6 mm, between 6 mm to 10 mm, and greater than 10 mm, respectively. In general, light precipitation rarely can reach the soil zone deeper than 40 cm because of evaporation, thus it makes almost no contribution to DSR (Zhang et al., 2016). Such a classification may be revised under different vegetation covering conditions in different regions (Kosmas et al., 2000).

According to this classification, statistics of moderate to strong precipitation events and their percentage shares in the annual precipitation from 2013 to 2015 are shown in Table 2. In 2013, there are only two precipitation events with intensity greater than 6 mm. The total amount of these two precipitation events is 43.4 mm, which represents 52.29% of the annual precipitation in 2013. In 2014, there are 11 precipitation events with intensity greater than 6 mm, much more frequent than that of 2013 (2 times) and moderately more frequent than that of 2015 (8 times). The total moderate to strong precipitation in 2014 is 98.6 mm, representing 47.96% of the annual precipitation in 2014. In 2015, there are 8 precipitation events with intensity greater than 6 mm, accounting for 53.54% of the annual precipitation in 2015.

Among these three years, 2015 has the largest percentage of moderate to strong precipitation over the annual precipitation. However, at this same year, one has seen the smallest ratio of annual DSR/precipitation ratio or annual recharge coefficient (see Table 1). This implies that the annual DSR does not seem to be positively correlated to the annual total precipitation. This finding has a few profound consequences. It basically states that assigning a constant annual

388 recharge coefficient for a particular soil regardless of precipitation patterns is not a good practice,
 389 because annual DSR is not always proportional to the total annual precipitation. Instead, it
 390 appears to be more closely related to individual precipitation events stronger than 10 mm.

391 Table 2: Percentage of valid precipitation in total precipitation amount.

Year	Number of precipitation >6mm (24 hr cumulative)	Amount of precipitation >6mm (mm)	Valid precipitation /annual precipitation (%)
2013	2	43.4	52.29
2014	11	98.6	47.96
2015	8	99.8	53.54

392

393 Table 3 lists the number of strong precipitation (with amount greater than 10 mm) and also
 394 the strongest precipitation amount for each of 2013, 2014 and 2015. In 2013, there are only 2
 395 strong precipitation events, but the maximum single-day precipitation amount reaches 32 mm
 396 (August 3). The accumulative strong precipitation of 2013 is 43.4 mm, which is 52.28% of the
 397 annual precipitation in 2013. In 2014, there are 4 strong precipitation events and the maximum
 398 single-day precipitation amount is 15 mm. The accumulative strong precipitation of 2014 is 49.6
 399 mm, which is 24.12% of the annual precipitation in 2014. In 2015, there are 6 strong
 400 precipitation events, and the maximum single-day precipitation amount is 17.2 mm. The
 401 accumulative strong precipitation of 2015 is 86.6 mm, which represents 46.46% of the annual

402 precipitation in 2015. The annual DSR versus annual precipitation ratios are 24.33%, 10%, and
403 4.94% for 2013, 2014, and 2015, respectively.

404 As shown in Table 3, the strongest single-day precipitation (32 mm in 2013) appears to
405 affect DSR the most in 2013. For 2014 and 2015, as the strongest precipitation events in these
406 two years are significantly smaller than that in 2013. Such a positive correlation is particularly
407 strong for 2013 which has the largest maximum precipitation event of 32 mm, showing that the
408 strong single-day precipitation affects DSR. This positive correlation is weaker for 2014 and
409 2015 which have moderate and somewhat similar maximum precipitation events (15 mm and
410 17.2 mm, respectively). As shown in Figures 4 and 5, precipitation patterns in 2014 and 2015 are
411 quite different despite the fact that the maximum precipitation events are similar to each other.
412 The precipitation in 2014 is somewhat uniformly distributed from April to November, while the
413 precipitation in 2015 is mostly concentrated from May to June. This observation suggests that
414 DSRs for these two years are related to the precipitation pattern as well as the precipitation
415 strength. However, precisely quantifying such a correlation between DSR and the precipitation
416 pattern and precipitation strength requires further investigations.

417 In summary, one may conclude that annual DSR in arid and semi-arid regions mainly rely
418 on strong precipitation events, but the determination of the threshold for strong precipitation
419 events that directly contribute to DSR is still unclear and requires further investigation.

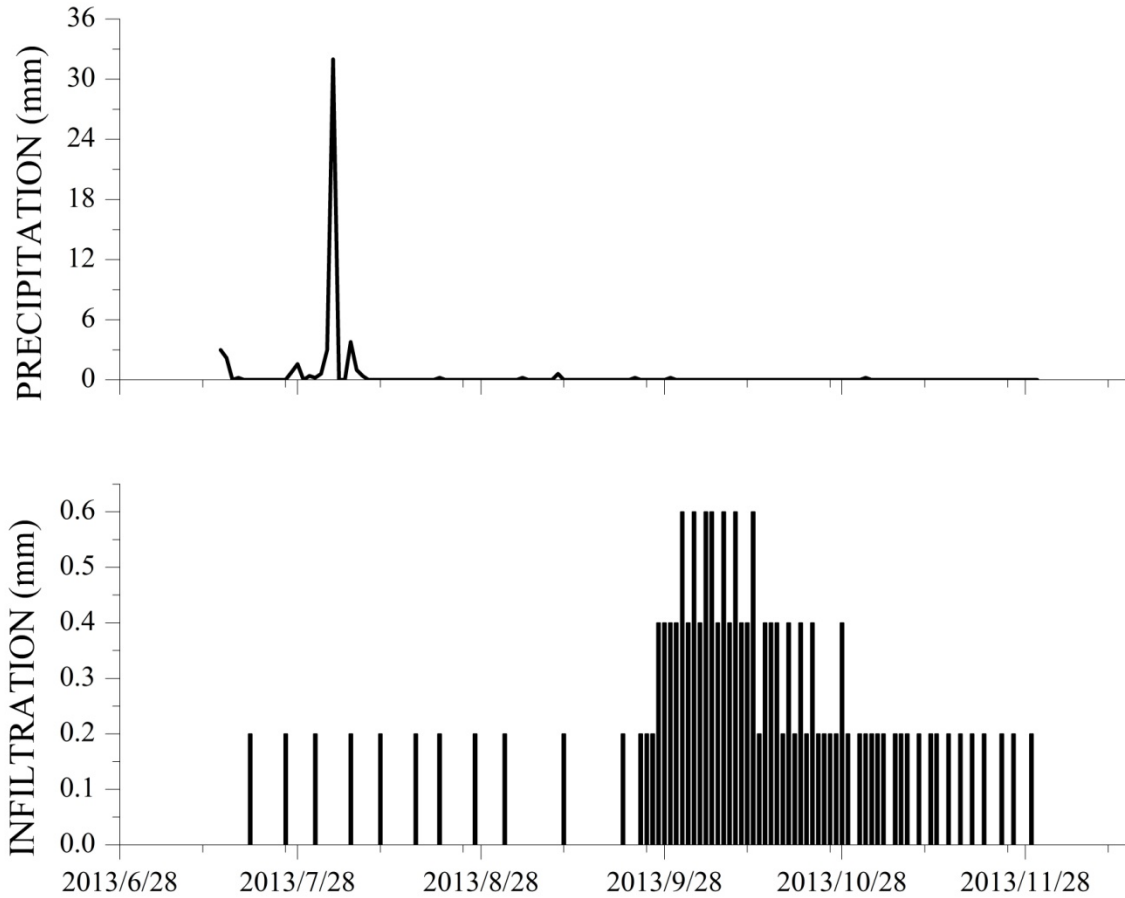
420 Table 3: Inter-annual statistics of strong precipitation and its percentage in total annual
421 precipitation amount.

Year	Number of strong precipitation	Maximum precipitation	Annual DSR (mm)	Annual DSR /annual precipitation (%)
------	--------------------------------	-----------------------	-----------------	--------------------------------------

event(mm)				
2013	2	32	20.2	24.33
2014	4	15	20.6	10
2015	6	17.2	9.2	4.94

422

423 Under the condition of continuous precipitation, it may be difficult to discretize
424 precipitation into individual events. The following example illustrates a procedure to deal with
425 this situation. As shown in Figure 6, there is a 13-days continuous precipitation process in 2013
426 from July 27 to August 8, and the accumulative precipitation is 43.8 mm. The start of a
427 continuous DSR distribution corresponding to this 13-day continuous precipitation event is
428 observed 3 days after the end of this precipitation process, and the peak value of DSR occurs 46
429 days after the end of this precipitation process. The DSR distribution gradually recedes to zero
430 around 78 days after the end of the precipitation process. The accumulative DSR amount over a
431 75-day period is 18.4 mm. The ratio of the 75-day cumulative DSR over the 13-day precipitation
432 event is 42%.



433
434 Figure 6: One-day intensive precipitation's contribution to DSR in 2013.

435 **4. Discussion**

436 This improved lysimeter is on the real-time dynamic monitoring of DSR, and it provides
 437 reliable evidence for an accurate evaluation of precipitation-related recharging capability of bare
 438 sand lands in arid and semi-arid regions. However, there are a number of issues that deserves
 439 further attention and requires additional investigations in the future. The moisture evaporation,
 440 the soil absorption of moisture, and the water infiltration of post-evaporative redistribution, are
 441 all very complex processes, especially in arid and semi-arid regions. It is sometimes difficult to
 442 clearly distinguish the amount of evaporation and DSR with conventional methods as outlined in
 443 the introduction. This study selects precipitation and infiltration data during the period from
 444 April 1 to November 30, so the influence of freeze-thaw process during winter is avoided, and

445 the experimental design and data analysis is simplified. For this reasons, the next steps should be
446 a full-term monitoring, a systematic study on DSR, as well as a study on the soil temperature and
447 daily temperature influences on DSR.

448 Although this experiment does not address the issue of soil temperature effect on DSR in
449 great details, the relationship between DSR and soil temperature is evident. In general, a higher
450 temperature means a stronger evaporation demand, thus an often smaller DSR.

451 Through the analysis of this study, one can see that the use of an annual recharge coefficient
452 for the study area is not supported by the data collected from the new lysimeter, as the annual
453 recharge is not positively correlated with the annual total precipitation. Instead, we find that the
454 recharge is somewhat positively correlated with a few strong precipitation events (greater than
455 10 mm), and is closely correlated with the strongest precipitation event (considerably greater
456 than 10 mm), as well as the precipitation patterns. It is probably reasonable to assign different
457 weighting factors for different precipitation strengths to calculate DSR. However, the threshold
458 to define a strong precipitation event that makes direct contribution to DSR is not precisely
459 quantified, and this is a subject that should be investigated in more details in the future. The
460 determination of weighting factors for different precipitation strengths is also a subject requires
461 further investigation.

462 This investigation is based on detailed analysis of precipitation and DSR data at the study
463 site without involving modeling effort which certainly will be explored in the future as well. This
464 study represents our first attempt of questioning the application of recharge coefficient concept
465 in arid and semi-arid regions.

466

467 **5. Conclusions**

468 This study uses a newly designed lysimeter to study three consecutive years (2013-2015) of DSR
469 underneath bare sand land on the Eastern margin of Mu Us Sandy Land in the Ordos basin of
470 China. The objective is to identify the characteristics of the DSR distribution and the factors
471 affecting the DSR distribution. Specifically, we like to examine if the commonly used recharge
472 coefficient concept can be applied for arid and semi-arid regions such as the Eastern margin of
473 Mu Us Sandy Land of China. The following conclusions can be drawn from this study:
474 (1) The annual recharge coefficient concept is generally inapplicable for estimating DSR in the
475 study site.
476 (2) Precipitation pattern including precipitation intensity and precipitation season significantly
477 influences DSR.
478 (3) The temperature influences the DSR/precipitation ratio, which is less in summer as in other
479 seasons, given the similar precipitation intensity.
480 (4) DSR is not correlated with the annual precipitation. Instead, it is correlated with the strong
481 precipitation (greater than 10 mm) events at the site. However, quantitative determination of
482 the thresholds for such strong precipitation events that makes direct contribution to DSR is
483 not entirely understood. Further investigation is needed on this subject.

484

485 **Acknowledgements.** This study was supported with research grants from the Ministry of
486 Science and Technology of the People's Republic of China (2013CB429901).

487

488 **References**

489

490 Acworth, R. I., Rau, G. C., Cuthbert, M. O., Jensen, E., and Leggett, K.: Long-term spatio-temporal
491 precipitation variability in arid-zone Australia and implications for groundwater recharge, *Hydrogeology*
492 *Journal*, 24, 905-921, 2016.

493 Adolph, E. F.: *Physiology of Man in the Desert*, Physiology of Man in the Desert., 1947.

494 Allison, G., Gee, G., and Tyler, S.: Vadose-zone techniques for estimating groundwater recharge in arid
495 and semiarid regions, *Soil Science Society of America Journal*, 58, 6-14, 1994.

496 Allocca, V., Manna, F., and De Vita, P.: Estimating annual groundwater recharge coefficient for karst
497 aquifers of the southern Apennines (Italy), *Hydrology and Earth System Sciences*, 18, 803, 2014.

498 Arnold, J. G., Moriasi, D. N., Gassman, P. W., Abbaspour, K. C., White, M. J., Srinivasan, R., Santhi, C.,
499 Harmel, R., Van Griensven, A., and Van Liew, M. W.: SWAT: Model use, calibration, and validation,
500 *Transactions of the ASABE*, 55, 1491-1508, 2012.

501 Beatley, J. C.: Phenological events and their environmental triggers in Mojave Desert ecosystems,
502 *Ecology*, 55, 856-863, 1974.

503 Collins, S. L., Belnap, J., Grimm, N., Rudgers, J., Dahm, C. N., D'odorico, P., Litvak, M., Natvig, D., Peters, D.
504 C., and Pockman, W.: A multiscale, hierarchical model of pulse dynamics in arid-land ecosystems, *Annual
505 Review of Ecology, Evolution, and Systematics*, 45, 397-419, 2014.

506 Duncan, M., Srinivasan, M., and McMillan, H.: Field measurement of groundwater recharge under
507 irrigation in Canterbury, New Zealand, using drainage lysimeters, *Agricultural Water Management*, 166,
508 17-32, 2016.

509 Farahani, H., Howell, T., Shuttleworth, W., and Bausch, W.: Evapotranspiration: progress in
510 measurement and modeling in agriculture, *Trans. Asabe*, 50, 1627-1638, 2007.

511 Fayer, M. J.: UNSAT-H version 3.0: Unsaturated soil water and heat flow model. Theory, user manual,
512 and examples, Pacific Northwest National Laboratory, 13249, 2000.

513 Fiorillo, F., Pagnozzi, M., and Ventafridda, G.: A model to simulate recharge processes of karst massifs,
514 *Hydrological Processes*, 29, 2301-2314, 2015.

515 Fritzsche, A., Pagels, B., and Totsche, K. U.: The composition of mobile matter in a floodplain topsoil: A
516 comparative study with soil columns and field lysimeters, *Journal of Plant Nutrition and Soil Science*, 179,
517 18-28, 2016.

518 Gee, G. W., and Hillel, D.: Groundwater recharge in arid regions: review and critique of estimation
519 methods, *Hydrological Processes*, 2, 255-266, 1988.

520 Glenn, E. P., Anday, T., Chaturvedi, R., Martinez-Garcia, R., Pearlstein, S., Soliz, D., Nelson, S. G., and
521 Felger, R. S.: Three halophytes for saline-water agriculture: An oilseed, a forage and a grain crop,
522 *Environmental and Experimental Botany*, 92, 110-121, 2013.

523 Goldhamer, D. A., Fereres, E., Mata, M., Girona, J., and Cohen, M.: Sensitivity of continuous and discrete
524 plant and soil water status monitoring in peach trees subjected to deficit irrigation, *Journal of the
525 American Society for Horticultural Science*, 124, 437-444, 1999.

526 Good, S. P., Noone, D., and Bowen, G.: Hydrologic connectivity constrains partitioning of global
527 terrestrial water fluxes, *Science*, 349, 175-177, 2015.

528 Hickel, K., and Zhang, L.: Estimating the impact of rainfall seasonality on mean annual water balance
529 using a top-down approach, *Journal of Hydrology*, 331, 409-424, 2006.

530 Howell, T. A., Schneider, A. D., and Jensen, M. E.: History of lysimeter design and use for
531 evapotranspiration measurements, *Lysimeters for Evapotranspiration and Environmental
532 Measurements*, 1991, 1-9,

533 Huxman, T. E., Snyder, K. A., Tissue, D., Leffler, A. J., Ogle, K., Pockman, W. T., Sandquist, D. R., Potts, D.
534 L., and Schwinning, S.: Precipitation pulses and carbon fluxes in semiarid and arid ecosystems, *Oecologia*,
535 141, 254-268, 2004.

536 Jiménez-Martínez, J., Candela, L., Molinero, J., and Tamoh, K.: Groundwater recharge in irrigated semi-
537 arid areas: quantitative hydrological modelling and sensitivity analysis, *Hydrogeology Journal*, 18, 1811-
538 1824, 2010.

539 Kalbus, E., Reinstorf, F., and Schirmer, M.: Measuring methods for groundwater? surface water
540 interactions: a review, *Hydrology and Earth System Sciences Discussions*, 10, 873-887, 2006.

541 Karnieli, A., Qin, Z., Wu, B., Panov, N., and Yan, F.: Spatio-temporal dynamics of land-use and land-cover
542 in the Mu Us sandy land, China, using the change vector analysis technique, *Remote Sensing*, 6, 9316-
543 9339, 2014.

544 Katz, B. S., Stotler, R. L., Hirmas, D., Ludvigson, G., Smith, J. J., and Whittemore, D. O.: Geochemical
545 Recharge Estimation and the Effects of a Declining Water Table, *Vadose Zone Journal*, 15, 2016.

546 Klaus, J., and McDonnell, J.: Hydrograph separation using stable isotopes: review and evaluation, *Journal*
547 *of Hydrology*, 505, 47-64, 2013.

548 Kosmas, C., Danalatos, N., and Gerontidis, S.: The effect of land parameters on vegetation performance
549 and degree of erosion under Mediterranean conditions, *Catena*, 40, 3-17, 2000.

550 Krysanova, V., Hattermann, F., and Wechsung, F.: Development of the ecohydrological model SWIM for
551 regional impact studies and vulnerability assessment, *Hydrological Processes*, 19, 763-783, 2005.

552 Li, X., Zhang, Z., Tan, H., Gao, Y., Liu, L., and Wang, X.: Ecological restoration and recovery in the wind-
553 blown sand hazard areas of northern China: relationship between soil water and carrying capacity for
554 vegetation in the Tengger Desert, *Science China. Life Sciences*, 57, 539, 2014.

555 Li, X. R., Ma, F. Y., Xiao, H. L., Wang, X. P., and Kim, K. C.: Long-term effects of revegetation on soil water
556 content of sand dunes in arid region of Northern China, *Journal of Arid Environments*, 57, 1-16, 2004.

557 Liu, Q., Yasufuku, N., Miao, J., and Ren, J.: An approach for quick estimation of maximum height of
558 capillary rise, *Soils and Foundations*, 54, 1241-1245, 2014.

559 Ma, J., Ding, Z., Edmunds, W. M., Gates, J. B., and Huang, T.: Limits to recharge of groundwater from
560 Tibetan plateau to the Gobi desert, implications for water management in the mountain front, *Journal of*
561 *Hydrology*, 364, 128-141, 2009.

562 McWhorter, D. B., and Sunada, D. K.: Ground-water hydrology and hydraulics, *Water Resources*
563 *Publication*, 1977.

564 Min, L., Shen, Y., Pei, H., and Jing, B.: Characterizing deep vadose zone water movement and solute
565 transport under typical irrigated cropland in the North China Plain, *Hydrological Processes*, 2017.

566 Modarres, R., and da Silva, V. d. P. R.: Rainfall trends in arid and semi-arid regions of Iran, *Journal of Arid*
567 *Environments*, 70, 344-355, 2007.

568 Nyman, P., Sheridan, G. J., Smith, H. G., and Lane, P. N.: Modeling the effects of surface storage,
569 macropore flow and water repellency on infiltration after wildfire, *Journal of Hydrology*, 513, 301-313,
570 2014.

571 Ogle, K., and Reynolds, J. F.: Plant responses to precipitation in desert ecosystems: integrating functional
572 types, pulses, thresholds, and delays, *Oecologia*, 141, 282-294, 2004.

573 Postma, D., Boesen, C., Kristiansen, H., and Larsen, F.: Nitrate reduction in an unconfined sandy aquifer:
574 water chemistry, reduction processes, and geochemical modeling, *Water Resources Research*, 27, 2027-
575 2045, 1991.

576 Ritsema, C. J., and Dekker, L. W.: How water moves in a water repellent sandy soil: 2. Dynamics of
577 fingered flow, *Water Resources Research*, 30, 2519-2531, 1994.

578 Sanford, W.: Recharge and groundwater models: an overview, *Hydrogeology Journal*, 10, 110-120, 2002.

579 Scanlon, B. R.: Evaluation of methods of estimating recharge in semiarid and arid regions in the
580 southwestern US, *Groundwater recharge in a desert environment: The southwestern United States*, 235-
581 254, 2013.

582 Schymanski, S. J., Sivapalan, M., Roderick, M., Beringer, J., and Hutley, L.: An optimality-based model of
583 the coupled soil moisture and root dynamics, *Hydrology and Earth System Sciences Discussions*, 12, 913-
584 932, 2008.

585 Shou, W., Musa, A., Liu, Z., Qian, J., Niu, C., and Guo, Y.: Rainfall partitioning characteristics of three
586 typical sand-fixing shrubs in Horqin Sand Land, north-eastern China, *Hydrology Research*, nh2016177,
587 2016.

588 Šimůnek, J., Van Genuchten, M. T., and Šejna, M.: HYDRUS: Model use, calibration, and validation, *Trans.*
589 *Asabe*, 55, 1261-1274, 2012.

590 Soyly, M., Istanbuluoglu, E., Lenters, J., and Wang, T.: Quantifying the impact of groundwater depth on
591 evapotranspiration in a semi-arid grassland region, *Hydrology and Earth System Sciences*, 15, 787-806,
592 2011.

593 Stessel, R., and Murphy, R.: A lysimeter study of the aerobic landfill concept, *Waste Management &*
594 *Research*, 10, 485-503, 1992.

595 Turkeltaub, T., Kurtzman, D., Bel, G., and Dahan, O.: Examination of groundwater recharge with a
596 calibrated/validated flow model of the deep vadose zone, *Journal of Hydrology*, 522, 618-627, 2015.

597 van Dam, J. C.: Field-scale water flow and solute transport: SWAP model concepts, parameter estimation
598 and case studies, [sn], 2000.

599 Vauclin, M., Khanji, D., and Vachaud, G.: Experimental and numerical study of a transient,
600 two-dimensional unsaturated-saturated water table recharge problem, *Water Resources Research*, 15,
601 1089-1101, 1979.

602 Voeckler, H. M., Allen, D. M., and Alila, Y.: Modeling coupled surface water–Groundwater processes in a
603 small mountainous headwater catchment, *Journal of Hydrology*, 517, 1089-1106, 2014.

604 Weihermüller, L., Siemens, J., Deurer, M., Knoblauch, S., Rupp, H., Göttlein, A., and Pütz, T.: In situ soil
605 water extraction: a review, *Journal of environmental quality*, 36, 1735-1748, 2007.

606 Williams, W. D.: Salinisation: A major threat to water resources in the arid and semi-arid regions of the
607 world, *Lakes & Reservoirs: Research & Management*, 4, 85-91, 1999.

608 Wu, B., and Ci, L. J.: Landscape change and desertification development in the Mu Us Sandland,
609 Northern China, *Journal of Arid Environments*, 50, 429-444, 2002.

610 Zhang, J., Felzer, B. S., and Troy, T. J.: Extreme precipitation drives groundwater recharge: the Northern
611 High Plains Aquifer, central United States, 2016.

612 Zhang, L., Dawes, W., and Walker, G.: Response of mean annual evapotranspiration to vegetation
613 changes at catchment scale, *Water resources research*, 37, 701-708, 2001.

614 Zhang, Y., Kendy, E., Qiang, Y., Changming, L., Yanjun, S., and Hongyong, S.: Effect of soil water deficit on
615 evapotranspiration, crop yield, and water use efficiency in the North China Plain, *Agricultural Water*
616 *Management*, 64, 107-122, 2004.

617 Zhang, Z.-S., Liu, L.-C., Li, X.-R., Zhang, J.-G., He, M.-Z., and Tan, H.-J.: Evaporation properties of a
618 revegetated area of the Tengger Desert, North China, *Journal of arid Environments*, 72, 964-973, 2008.

619 Zhou, J., Fu, B., Gao, G., Lü, Y., Liu, Y., Lü, N., and Wang, S.: Effects of precipitation and restoration
620 vegetation on soil erosion in a semi-arid environment in the Loess Plateau, China, *Catena*, 137, 1-11,
621 2016.

622